Food Innovation and Advances

ARTICLE

Open Access

https://doi.org/10.48130/fia-0026-0002

Food Innovation and Advances **2026**, 5(1): 64–75

Enhanced production of ferulic acid and *p*-coumaric acid through optimized autohydrolysis pretreatment coupled with a dual-enzyme system of xylanase and feruloyl esterase for efficient corncob enzymatic hydrolysis

Jinghao Ma[1], Xiaoyan Liu[1], Rana Abdul Basit[1], Lin Xiao[3], Peng Gao[1], Wenqi Cui[1], Ming Chen[1], Zhilei Fu[4], Jinlong Yan[3], Yuchun Liu[5*] and Guangsen Fan[1,2*]

[1] *Key Laboratory of Geriatric Nutrition and Health (Beijing Technology and Business University), Ministry of Education, Beijing 100048, China*
[2] *Guangxi Key Lab of Agricultural Resources Chemistry and Biotechnology, College of Chemistry and Food Science, Yulin Normal University, Yulin, Guangxi 537000, China*
[3] *Shandong Longlive Bio-technology Public Limited Company, Dezhou, Shandong 251200, China*
[4] *School of Biology and Food Science, Hebei Minzu Normal University, Chengde, Hebei 067000, China*
[5] *Academy of National Food and Strategic Reserves Administration, Beijing 100037, China*
* Correspondence: lyc@ags.ac.cn (Liu Y); fanguangsen@btbu.edu.cn (Fan G)

Abstract

This study aims to enhance the utilization value of corncob by efficiently extracting ferulic acid (FA) and *p*-coumaric acid (*p*CA) through environmentally sustainable methods. The research explores a novel approach that combines autohydrolysis pretreatment with the synergistic effects of xylanase SrXyn10AR and feruloyl esterase BpFae$^{T132C\text{-}D143C}$. By conducting comprehensive optimization through single-factor analysis and response surface methodology (RSM) experiments, the optimal processing conditions were established: corncob particles of 40–60 mesh size were subjected to autohydrolysis at 165 °C for 34 min with a solid-to-liquid ratio of 1:90.8, followed by enzymatic hydrolysis at 43 °C, 90 rpm, and pH 5.5 for 2.5 h, utilizing BpFae$^{T132C\text{-}D143C}$ and SrXyn10AR enzymes at a concentration of 1.1 U/mL each. Under these refined conditions, the yield of FA and *p*CA soared to 63.42%, marking a 2.42-fold increase compared to pre-optimization levels. Furthermore, this process yielded xylooligosaccharides as a valuable co-product, with a yield of 303.31 mg/g. In conclusion, this study develops an efficient and environmentally friendly strategy for extracting phenolic acids from corncob. By leveraging autohydrolysis pretreatment combined with dual-enzyme hydrolysis technology, this approach can pave a new way for the value-added utilization of corncob resources.

Citation: Ma J, Liu X, Basit RA, Xiao L, Gao P, et al. 2026. Enhanced production of ferulic acid and *p*-coumaric acid through optimized autohydrolysis pretreatment coupled with a dual-enzyme system of xylanase and feruloyl esterase for efficient corncob enzymatic hydrolysis. *Food Innovation and Advances* 5(1): 64–75 https://doi.org/10.48130/fia-0026-0002

Introduction

Corn is the second most cultivated crop globally, with production levels reaching an impressive 1.2 billion tons[1,2]. The generation of substantial quantities of inexpensive corncob by-products invariably accompanies the production of corn. Studies have indicated that for every ton of processed corn, approximately 0.3 tons of corncob by-products are generated, resulting in an estimated annual worldwide production of approximately 363 million tons of corncob[3]. For an extended period, these substantial quantities of corncob have remained underutilized, with the majority being discarded or utilized solely as fuel and basic animal feed. This has led to significant environmental pollution and the squandering of valuable renewable resources[4]. In response to the challenges posed by global warming, most countries worldwide have embraced and are actively implementing strategies for carbon neutrality and carbon peaking[5]. Given this context, it is imperative to research more efficient utilization methods for corncob, which constitutes an abundant renewable resource.

Research has demonstrated that corncob is highly enriched with cellulose (35%–40%), hemicellulose (32%–36%), and lignin (17%–20%)[6,7]. Effective utilization of these three primary components is crucial for achieving high-value and high-quality applications of corncob. Various studies have successfully investigated the production of dietary fiber, xylooligosaccharide (XOS), fuel ethanol, and other valuable products from the components present in corncob. A prevalent challenge in these research endeavors is the effective breakdown of the complex and dense lignocellulosic structure[8]. The difficulty in disintegrating the lignocellulosic structure of corncob is primarily due to the organized arrangement of its crystalline fibers. Additionally, the presence of phenolic acid compounds, which form cross-linkages between hemicellulose and lignin through ester or ether bonds, further reinforces this robust structure. This intertwining complicates the separation of these components. Consequently, the crucial aspect of effectively disintegrating lignocellulose lies in breaking the ester and ether bonds that link these components together. To tackle this issue, pretreatment methods, including autohydrolysis, steam explosion, and alkaline extraction, are utilized for processing agricultural waste[7,9]. A primary objective of these pretreatment processes is to disrupt the ester and ether bonds. Through these pretreatments, not only can dietary fiber, XOS, xylose, and glucose be efficiently extracted, but also small quantities of phenolic compounds such as ferulic acid (FA) and *p*-coumaric acid (*p*CA) are generated. These phenolic compounds possess excellent antioxidant and anti-inflammatory properties, making them valuable in the pharmaceutical, cosmetic, and food industries[10,11].

Research has shown that corncob is a type of agricultural waste that is particularly rich in phenolic acids, especially FA and *p*CA. The concentrations of FA (1.4%) and *p*CA (1%–2%) in corncob are higher

compared to other agricultural wastes like wheat bran, wheat straw, bagasse, peanut shells, and corn stover, which typically contain between 0.4%–1.2% of these acids[10]. Employing targeted technologies to cleave the phenolic acid-derived ester or ether bonds in corncob allows for the efficient extraction of valuable compounds like FA and *p*CA, which have important applications in pharmaceuticals and other industries. Furthermore, this approach enhances the potential for the resource utilization of the remaining corncob residue, whose cross-linked structure has been disrupted[10,12]. This strategy offers an effective pathway for the gradual disintegration and comprehensive exploitation of corncob resources.

Currently, alkaline hydrolysis serves as the primary method for obtaining FA and *p*CA from corncob. While effective in breaking ester and ether bonds within lignin-polysaccharide complexes to release substantial phenolic acids, this method requires large solvent volumes and generates significant alkaline wastewater, exacerbating environmental pollution and potentially damaging functional groups[13–15]. In contrast, bio-enzymatic methods have gained preference due to mild conditions, environmental compatibility, energy efficiency, and high specificity. This approach employs specific enzymes to cleave ether or ester bonds, selectively releasing FA and *p*CA[16]. Feruloyl esterase (FAE) is an enzyme that specifically targets and cleaves the ester bond linking hydroxycinnamic acids to sugars, thereby enabling the degradation of phenolic acids in waste biomass without compromising other valuable chemical components. Regrettably, the intricate lignocellulosic structure of corncob poses a challenge, rendering the highly specific FAE unable to reach the ether-ester bonds nestled deep within this dense matrix. Consequently, preprocessing steps, including autohydrolysis, become indispensable to efficiently break down the ester linkages between FA, *p*CA, and the hemicellulose backbone within the corncob lignocellulose. This process enables FAE to liberate FA and *p*CA effectively[11,17]. Biomass enzymatic conversion typically requires multi-enzyme synergy due to structural complexity[18,19]. Although FAE alone can partially cleave ester bonds, core lignocellulose components remain largely intact, hindering enzyme access. Xylanase supplementation enhances FAE effectiveness by degrading hemicellulose main chains, disrupting the structural framework, and facilitating FAE access to side-chain esters. This synergistic action creates a cycle where main-chain degradation promotes side-chain release and vice versa, significantly improving FA and *p*CA yields[20].

In view of this, this paper embraces the principles of efficiency and environmental sustainability by adopting autohydrolysis, a prevalent pretreatment technique for agricultural waste, to treat corncob. Following this, leveraging the highly potent FAE and xylanase, which were previously developed by the research team, for synergistic enzymatic hydrolysis, a technology was devised that efficiently processes corncob to yield FA and *p*CA, thereby paving a novel avenue for the high-value application of corncob.

Materials and methods

Materials

The corncob utilized in this study was generously provided by Shandong Longlive Bio-technology Co., Ltd, and was stored in a dry environment. Ampicillin, kanamycin, isopropyl-*β*-D-thiogalactopyranoside (IPTG), beechwood xylan, the FA standard, and the *p*CA standard were procured from Sigma-Aldrich® (Beijing, China). Additionally, ferulic acid methylester, acetonitrile (HPLC grade), and methanol (HPLC grade) were sourced from Beijing Mreda Technology Co., Ltd. Unless specified otherwise, all other chemicals were of analytical grade and readily available commercially.

Production and activity analysis of FAE pGEX-4T-1-BpFae$^{T132C-D143C}$

The FAE variant, designated as pGEX-4T-1-BpFae$^{T132C-D143C}$, derived from the *Burkholderia pyrrocinia* FAE BpFae, was expressed in *Escherichia coli* (*E. coli*) within the laboratory setting[21]. Enzyme activity was assessed according to the previously established methods, conducted at 50 °C and pH 5.5 using a 1 mmol/L solution of ferulic acid methyl ester prepared in 50% dimethylsulfoxide (DMSO)[21]. One unit (U) of BpFae$^{T132C-D143C}$ activity was defined as the quantity of crude enzyme capable of liberating 1 μmol of FA per minute under the conditions mentioned above.

Production and activity analysis of xylanase SrXyn10AR

The thermostable xylanase variant, SrXyn10AR, derived from *Streptomyces rameus* L2001 xylanase XynA, was expressed in *E. coli* according to a previous work[22,23]. The enzymatic activity of SrXyn10AR was evaluated at 50 °C and pH 5.5 using 225 μL of a 1% (w/v) beechwood xylan solution, according to the methodology described by Bailey et al.[24]. One unit (U) of SrXyn10AR activity was defined as the amount of crude enzyme required to produce 1 μmol of xylose equivalent per minute under the specified assay conditions.

Chemical characterization of corncob

The corncob was ground and sieved, with the 40–60 mesh particles selected for compositional analysis. The moisture content of corncob was determined by comparing the weight before and after drying at 105 °C[25]. The protein content was analyzed using the Kjeldahl method[25]. Ash content was measured by weighing the samples before and after heat treatment at 550 °C in a muffle furnace, as described in AOAC method 923.03[26]. Starch content was determined using the α-amylase method, in line with the AOAC method 996.11[26]. The total carbohydrates in the destarched corncob were quantified following the protocol described by the National Renewable Energy Laboratory (NREL)[27]. Briefly, 300 mg of corncob was hydrolyzed with 3 mL of 72% (w/w) sulfuric acid at 30 °C for 1 h, diluted to 4% (w/w) sulfuric acid, and autoclaved at 121 °C for 1 h. Subsequently, the fractions were filtered to separate the insoluble lignin from the solution. The monomeric sugar content in the hydrolysate was analyzed by high-performance liquid chromatography (HPLC, Water Corp., Milford, MA, USA) with a refractive index detector to quantify cellulose and hemicellulose[28]. The acid-soluble lignin content was determined spectrophotometrically at 320 nm using a UV-Vis spectrophotometer (TU-1901, Pgeneral, UV Spectrophotometer). In contrast, the insoluble lignin content was estimated gravimetrically by subtracting the residual ash weight from the total dry weight of the residual solid biomass after drying.

The determination of the alkali-extractable total FA and *p*CA content involved treating 0.5 g of corncob with 50 mL of a 2 mol/L sodium hydroxide solution at 50 °C for 4 h. The liquid fraction obtained from the alkaline treatment was separated from the solid residue by centrifuging at 12,000 rpm for 10 min. Following this, the liquor was neutralized using two volumes of 1 mol/L hydrochloric acid, preparing it for analysis by HPLC.

Autohydrolysis of corncob

Autohydrolysis of corncob was conducted in a 500 mL stainless-steel reactor (SLM500, Sen Long, Beijing, China). A mixture of 15 g of corncob (40–60 mesh) and 200 mL of deionized water was loaded into the reactor, where it was heated while being continuously stirred at 300 rpm using internal magnetic stirring. A PID controller precisely controlled the reaction temperature and time. Upon completion of the reaction, the reactor was swiftly cooled to 60 °C using tap water circulating through a cooling coil. The liquid fractions (LFs) were then separated from the residue by filtration, with the residue being washed several times with deionized water. The final volume of the liquid fraction, including wash water, and the weight of the lyophilized residue (LR) were recorded. Both were stored at −20 °C for subsequent enzymatic hydrolysis. Initial optimization of autohydrolysis parameters involved a single-factor design, examining various temperatures (120, 140, 160, 180, and 200 °C), times (20, 40, 60, 80, and 100 min), solid-to-liquid ratios (1:50, 1:60, 1:70, 1:80, 1:90, and 1:100), and corncob particle sizes (10–20, 20–40, 40–60, 60–80, and 80–100 mesh). Subsequently, response surface methodology (RSM) was employed to refine the autohydrolysis conditions further, focusing on three key factors: temperature, time, and solid-to-liquid ratio. The response value used for optimization was the yield of total FA and *p*CA (TFA*p*CA) after enzymatic hydrolysis of the autohydrolysis samples.

Enzymatic hydrolysis

Enzymatic hydrolysis was conducted on a 1-gram sample of LR. The quantity of LF required for each gram of LR was meticulously calculated to replicate the original ratio between LF and LR after autohydrolysis. The pH of the LF-LR mixture was then adjusted to 5.5 using a 50 mmol/L citric acid-sodium citrate buffer. Subsequently, BpFae$^{T132C\text{-}D143C}$ and SrXyn10AR enzymes were introduced to the LF-LR mixture, achieving final concentrations of 0.5 U/mL and 5 U/mL, respectively. The total volume was adjusted to 40 mL with the aforementioned buffer, and the mixture was then hydrolyzed for 2 h in a water bath shaker maintained at 40 °C and 90 rpm. Following hydrolysis, the reaction was promptly halted by placing the mixture in a boiling water bath for 10 min. Thereafter, HPLC analysis was immediately conducted to ascertain the concentrations of FA and *p*CA, enabling the calculation of the TFA*p*CA yield as per Eq. (1).

$$\mathrm{P(TFA}p\mathrm{CA)} = \frac{\text{The amount of FA and } p\text{CA released from corncob by treatment}}{\text{The amount of FA and } p\text{CA in original corncob}} \times 100\% \quad (1)$$

The impact of various conditions such as temperature (ranging from 25 to 45 °C in increments of 5 °C), shaking speed (from 60 to 180 rpm in increments of 30 rpm), pH (4.0 to 6.0 in increments of 0.5), BpFae$^{T132C\text{-}D143C}$ loading (0.125 to 2 U/mL in steps), the ratio of BpFae$^{T132C\text{-}D143C}$ to SrXyn10AR (5:1 to 1:20), and time (0.5 to 3.5 h in increments of 0.5 h) on the TFA*p*CA yield was evaluated through single-factor experiments. For further refinement, an RSM involving three key factors-temperature, time, and enzyme ratio-was implemented using Design-Expert Software 11.0 (StatEase Inc., Minneapolis, MN, USA).

To assess whether BpFae$^{T132C\text{-}D143C}$ and SrXyn10AR exhibit a synergistic effect during enzymatic hydrolysis, the TFA*p*CA yield was measured when pretreated corncob was hydrolyzed using BpFae$^{T132C\text{-}D143C}$ alone, SrXyn10AR alone, and a combination of both enzymes under the optimal conditions identified for autohydrolysis and enzymatic hydrolysis.

Analytical methods

The concentrations of FA and *p*CA were determined using an HPLC system (model 2695) equipped with a UV detector set at 320 nm. Samples were filtered through a 0.22 μm filter and applied to a chromatography system equipped with a ZORBAX Eclipse Plus C-18 column (4.6 I.D. x 250 mm, 5μm, Agilent, Palo Alto, CA). Separation was accomplished using a mobile phase composed of acetonitrile and 1% acetic acid solution (v/v) in a 2:8 ratio. The column oven temperature was maintained at 35 °C, and the separation process was completed within 30 min at a constant flow rate of 0.6 mL/min. A 10 μL injection volume was used for both samples and FA or *p*CA standards.

The concentrations of XOS, glucose, xylose, and arabinose were followed from the research of Qin et al.[29]. The yield of XOS, xylose, glucose, and arabinose (%, w/w) was calculated using Eq. (2).

$$\mathrm{P(X)(\%)} = \mathrm{C(X)(g/L)} \times \mathrm{V(L)} \times 100\%/\mathrm{W(g)} \quad (2)$$

where, P(X) is the XOS, xylose, arabinose, or glucose yield, C(X) represents the concentration of the respective component, V is the volume of the liquid fraction (LF), and W is the weight of the hemicellulose or cellulose in the corncob.

Scanning electron microscopy (SEM) and Fourier transform infrared (FTIR) were performed following the methodology described in a previous study[28].

Data analysis

Each treatment was conducted in triplicate, and the results were presented as the mean value ± standard deviation. The statistical significance of differences among the treatment groups was evaluated using a one-way ANOVA ($p < 0.05$), followed by Duncan's Multiple Comparison Test for multiple comparisons. The threshold *p*-value for significance was set at 0.05. The different letters (a, b, c, …) were used to express the significance when $p < 0.05$, and the same letter displayed there was no significance between groups ($p > 0.05$). Data analysis was performed using SPSS version 28.0 (IBM Corp., New York, USA), OriginPro version 9.1 (OriginLab, Northampton, MA, USA), Design-Expert version 11, and Microsoft Excel 2020 (Microsoft, USA).

Results and discussion

Composition of corncob

Corncob, which is a byproduct resulting from the corn processing industry, displays differences in its composition based on various factors, including corn variety and the specific processing methods employed[30]. As indicated in Supplementary Table S1, corncob was abundant in cellulose and hemicellulose, comprising 34.34% and 22.19% of its total composition, respectively. These observations were aligned well with the previously reported findings of Capetti et al.[31]. Thus, corncob emerged as a promising renewable resource for the manufacture of high-value products, including fuel ethanol and XOS. Furthermore, they comprised 16.26% lignin, 4.99% starch, 1.75% protein, and 4.18% ash. When employing the alkaline extraction method, the quantities of FA and *p*CA in corncob were precisely measured to be 17.8 and 11.29 mg/g, respectively. It was noteworthy that the concentrations of these acids could vary significantly depending on the source of the corncob and the processing methods employed (Table 1). Although the levels of FA and *p*CA vary significantly in corncob from different origins, it is generally abundant in phenolic acids. This abundance makes corncob a vital

Table 1. FA and *p*CA content in corncob across different studies.

FA (mg/g)	*p*CA (mg/g)	Ref.
14.05	21.12	[32]
14.50	35.10	[33]
10.13	–	[34]
18.80	–	[35]
–	10.66	[36]
17.8	11.29	In this study

resource for producing phenolic acid compounds that exhibit diverse biological functionalities. Moreover, the effective degradation of phenolic acids, such as FA, present in corncob will facilitate the enhanced utilization of their cellulose and hemicellulose fractions. To enhance efficiency in determining experimental conditions, future research endeavors will prioritize the yield of TFA*p*CA as the primary metric for evaluation.

Optimal conditions for autohydrolysis

Effect of autohydrolysis temperature on the yield of TFApCA

Autohydrolysis temperature critically determines lignocellulose disruption. Although minimal at lower temperatures, structural breakdown intensifies with rising temperature due to increased hydronium ions (H_3O^+) generation and accelerated degradation of inherent acids (e.g., acetic acid and FA). While higher temperatures enhance disruption, they may also degrade target products, necessitating optimization. As shown in Fig. 1a, TFA*p*CA yield from corncob showed a parabolic response to temperature, peaking at 6.79% at 160 °C. Below this optimum, incomplete structural breakdown limited FA and *p*CA release. Above 160 °C, free phenolic acids degraded into byproducts such as 4-vinylguaiacol and 4-vinylphenol[30,37]. This optimal temperature is substrate-dependent, varying from 175 °C for corn bran[30] to 60 °C for reed straws[38] due to structural differences among lignocellulosic materials. TFA*p*CA yield after enzymatic hydrolysis followed a similar trend, reaching 25.29% at 160 °C. Lower pretreatment temperatures limited enzyme accessibility and increased non-productive adsorption, while temperatures above 160 °C generated inhibitors that impaired BpFae$^{T132C\text{-}D143C}$ and SrXyn10AR activity[39,40]. Enzymatic treatment consistently outperformed the non-enzymatic control, confirming both enzymes' essential role. Residual enzyme activity exhibited a bell-shaped curve, peaking at 160 °C. This trend occurred because lower pretreatment temperatures inadequately disrupted the dense lignocellulosic structure of corncob, resulting in compact regions where macromolecules such as cellulose, hemicellulose, and lignin adsorbed the enzymes. However, when the autohydrolysis temperature surpassed 160 °C, the system may have accumulated excessively high concentrations of byproducts, such as acetic acid and furfural, which had inhibitory effects on the activities of the two enzymes[40,41].

Effect of autohydrolysis time on the yield of TFApCA

Autohydrolysis duration critically governs treatment intensity. Prolonged treatment at fixed temperature enhances structural disruption, breaking macromolecular polymers into basic units that further convert into furan derivatives (e.g., furfural, HMF) and organic acids like formic and levulinic acid[30,42]. As shown in Fig. 1b, TFA*p*CA yield from autohydrolysis alone fluctuated erratically with time, reflecting corncob heterogeneity and phenolic acid stability. Moderate durations released readily accessible bound FA and *p*CA, while extended treatment caused free phenolic acid degradation to

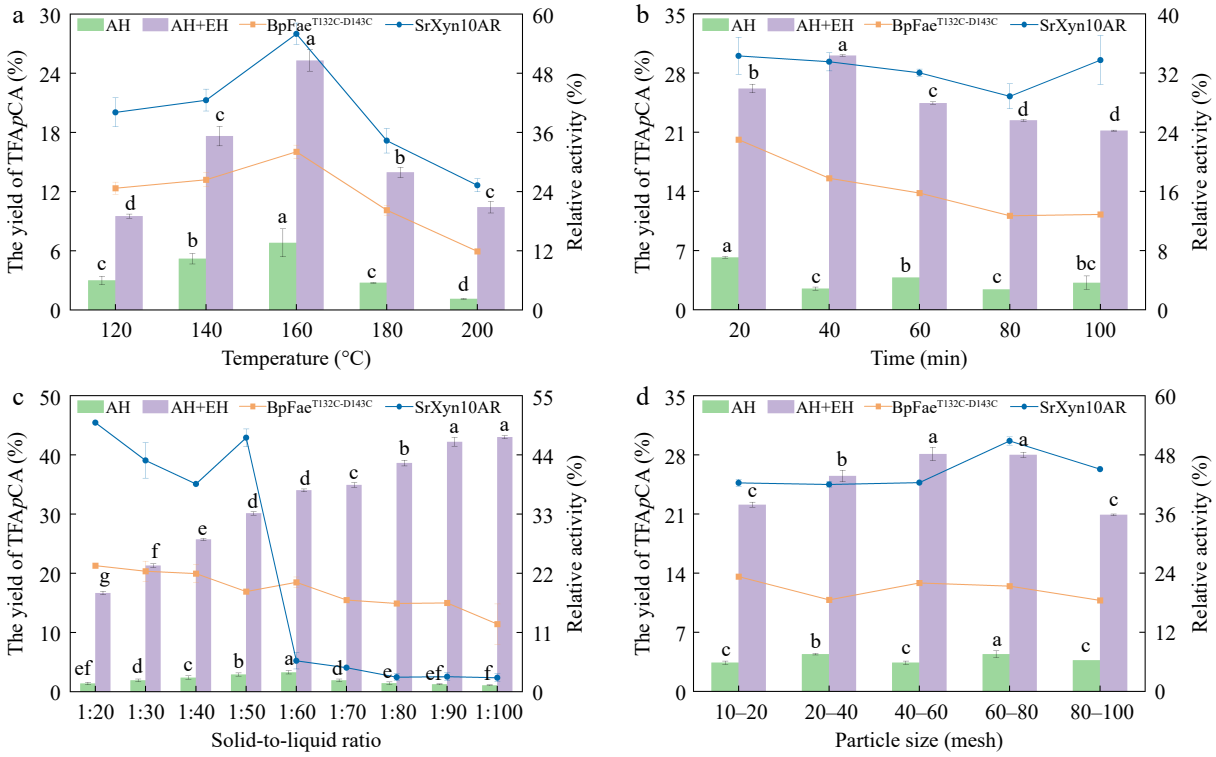

Fig. 1 Effects of (a) temperature, (b) time, (c) solid-to-liquid ratio, and (d) particle size on the yield of TFA*p*CA. AH, autohydrolysis only treatment, no enzymatic hydrolysis treatment; AH+EH, autohydrolysis plus enzymatic hydrolysis treatment. Squares, residual enzyme activity of BpFae$^{T132C\text{-}D143C}$; circles, residual enzyme activity of SrXyn10AR. Residual enzyme activity is defined as the ratio of the enzyme activity measured in the system to the initial enzyme activity.

outpace release from recalcitrant forms. Further increases in treatment intensity cause fluctuations in phenolic acid content due to the shifting balance between these two processes. Enzymatic hydrolysis of pretreated samples showed a distinct peak at 40 min (Fig. 1b). Shorter autohydrolysis provided insufficient structural disruption, while excessive durations generated enzymatic inhibitors[29]. The consistently higher yield from enzymatic treatment vs the control underscores the essential role of SrXyn10AR and BpFae$^{T132C-D143C}$. Residual enzyme activity generally declined with prolonged autohydrolysis due to cumulative inhibition. Interestingly, SrXyn10AR activity increased after 100 min, possibly due to the system's complex composition and evolving substrate properties.

Effect of solid-to-liquid ratio on the yield of TFApCA

The solid-to-liquid ratio critically determines corncob concentration, heat transfer efficiency, and concentrations of key catalytic species (e.g., H^+, H_3O^+, acetic acid) during autohydrolysis, thereby governing fiber disruption extent and subsequent enzymatic hydrolysis efficacy[28]. As shown in Fig. 1c, TFA*p*CA yield from autohydrolysis alone exhibited a parabolic response to the solid-to-liquid ratio. Low ratios limited active agent (e.g., H^+ and H_3O^+) concentration due to poor mixing and heat transfer, reducing lignocellulose disruption and yield. An optimal ratio of 1:60 enhanced FA and *p*CA release, while higher ratios promoted degradation of liberated phenolic acids into vanillin and 4-vinylguaiacol via excessive H_3O^+ generation. High ratios also dilute products, complicating separation and increasing wastewater treatment costs[43–45]. In contrast, during enzymatic hydrolysis with SrXyn10AR and BpFae$^{T132C-D143C}$, the TFA*p*CA yield increased with the solid-to-liquid ratio. Although harsher pretreatment degraded some free FA and *p*CA and generated inhibitors, the enhanced structural disruption overall improved enzyme access to the phenolic acid side chains, promoting a net release. However, the residual activity of both enzymes declined at ratios exceeding 1:60, with SrXyn10AR activity dropping to ~5%, indicating its particular susceptibility to the accumulated inhibitory compounds under intense conditions.

Effect of particle size on the yield of TFApCA

The particle size of lignocellulosic materials significantly influences TFA*p*CA yield by affecting specific surface area and internal structure. During autohydrolysis, particle size governs both the contact area with H_3O^+ and substrate accessibility for subsequent enzymatic hydrolysis[44]. As shown in Fig. 1d, TFA*p*CA yield from autohydrolysis alone showed no clear trend with particle size. This irregularity reflects competing effects: finer particles enhance surface area and FA/*p*CA release, but under intense conditions also promote degradation of liberated compounds, causing yield fluctuations[46]. After dual-enzyme hydrolysis, TFA*p*CA yield exhibited a distinct peak (28.10%) at 40–80 mesh. Moderate size reduction improved structural disruption and enzyme synergy, while excessively fine particles generated inhibitory substances that impaired enzyme activity[47]. Residual enzyme activity initially increased with smaller particle sizes due to enhanced substrate accessibility, then declined as inhibitors accumulated. The differing residual activity profiles of the two enzymes reflect their distinct properties and the complex corncob composition.

Optimization of autohydrolysis conditions using RSM for maximizing TFA*p*CA yield

Based on the single-factor experimental results, an RSM using the Box-Behnken design (BBD) was implemented. When optimizing other autohydrolysis conditions, the corncob mesh size ranges from 40–60 mesh, and the optimal mesh size also falls within this range. Therefore, this design focused on three key factors: temperature, time, and solid-to-liquid ratio. The experimental findings revealed notable disparities in the yield of TFA*p*CA after dual-enzyme hydrolysis among samples that underwent varying autohydrolysis treatments (Table 2). Notably, the lowest yield was observed in experiment group 2, totaling just 14.97%, whereas the highest yield was achieved in experiment group six, peaking at 44.96%. Utilizing Design-Expert software, a comprehensive multivariate regression analysis was conducted on the dataset comprising 15 experimental groups, ultimately yielding the following regression equation:

$$Y = 44.50 + 3.8562A - 3.0778B + 1.7763C - 7.2616AB + 0.0256AC - 0.2742BC - 12.6258A^2 - 8.1867B^2 - 11.2007C^2 \quad (3)$$

where, Y denotes the predicted response, specifically the yield of TFA*p*CA, while A, B, and C represent the factors of temperature, time, and solid-to-liquid ratio, respectively.

ANOVA confirmed the model's statistical significance ($p < 0.05$) with an insignificant lack-of-fit term ($p > 0.05$), indicating the regression equation accurately describes the factor-response relationship (Supplementary Table S2). The model demonstrated high reliability ($R^2 = 0.9949$), explaining 99.49% of data variance. Analysis of factor significance based on *F*-values and *p*-values identified temperature (A), time (B), and solid-to-liquid ratio (C) as influential parameters, with relative importance ranking A > B > C. This hierarchy aligns with previous autohydrolysis studies highlighting temperature and time as primary factors[28]. All quadratic terms significantly affected yield, while only the temperature-time interaction showed notable significance, consistent with established research[28].

Response surface analysis based on the regression equation revealed interactive effects of process factors on TFA*p*CA yield (Supplementary Fig. S1). The yield showed a parabolic response to increasing temperature (at fixed time, Supplementary Fig. S1a) or prolonged time (at fixed temperature), indicating both insufficient and excessive intensities reduce production. This pattern reflects the balance between lignocellulose disruption and byproduct formation: mild conditions incompletely release target compounds, while severe conditions generate inhibitory impurities that degrade FA and *p*CA. Similarly, low temperatures or solid-to-liquid ratios insufficiently disrupted the lignocellulosic structure, reducing yields

Table 2. The BBD and the responses of the dependent variables for autohydrolysis conditions.

Test No.	Temperature (°C)		Time (min)		Solid-to-liquid ratio		Yield of TFA*p*CA (%)
	A	Code A	B	Code B	C	Code C	
1	160	0	60	1	1:80	−1	20.77 ± 0.42
2	140	−1	40	0	1:80	−1	14.97 ± 0.37
3	140	−1	60	1	1:90	0	23.87 ± 0.24
4	160	0	20	−1	1:100	1	30.00 ± 0.30
5	160	0	20	−1	1:80	−1	25.00 ± 0.68
6	160	0	40	0	1:90	0	44.96 ± 0.07
7	140	−1	40	0	1:100	1	17.58 ± 0.05
8	160	0	60	1	1:100	1	24.67 ± 0.80
9	180	1	40	0	1:80	−1	23.72 ± 0.78
10	180	1	60	1	1:90	0	15.97 ± 0.58
11	180	1	20	−1	1:90	0	38.03 ± 0.58
12	180	1	40	0	1:100	1	26.43 ± 0.32
13	160	0	40	0	1:90	0	44.29 ± 0.69
14	140	−1	20	−1	1:90	0	16.88 ± 0.35
15	160	0	40	0	1:90	0	44.24 ± 0.89

(Supplementary Fig. S1b). Conversely, high ratios with elevated temperatures caused overtreatment, generating inhibitors that impaired enzymatic hydrolysis and degraded phenolic acids (Supplementary Fig. S1c). Extended autohydrolysis time or increased solid-to-liquid ratio also produced this parabolic trend due to competing structural disruption and impurity accumulation. Optimal conditions determined by Design-Expert 11 were 165 °C, 34 min, and a 1:90.8 solid-to-liquid ratio, predicting 45.48% TFA*p*CA yield. Experimental validation achieved 46.19% using a 40–60 mesh corncob, confirming model accuracy. The optimized process increased the yield 1.76-fold, demonstrating autohydrolysis conditions' significant impact on FA and *p*CA release.

Optimized conditions for enzymatic hydrolysis

Single factor

As shown in Fig. 2a, autohydrolyzed corncob residue liquor was further processed at 40 °C and 90 rpm for varying durations. The TFA*p*CA content in the supernatant showed a fluctuating trend, rising initially, then decreasing, before increasing again. This pattern reflects continuous adsorption and desorption of released FA and *p*CA between the solid residue and the liquid phase. Agitation initially promoted the transfer of retained phenolics into solution, followed by re-adsorption onto residues, with this cycle repeating until gradual equilibrium was approached[48]. Enzymatic treatment significantly enhanced TFA*p*CA yield compared to the non-enzymatic control. Yield increased with hydrolysis time up to 2.5 h before stabilizing. This improvement resulted from the synergistic action of BpFae$^{T132C\text{-}D143C}$ and SrXyn10AR, which hydrolyze feruloyl ester bonds in both solid and liquid phases. Beyond 2.5 h, product accumulation inhibited the enzymes, and their activity declined naturally, leading to yield stabilization[12]. Additionally, some ferulic acid groups remained trapped in compact, undegraded regions of the corncob, inaccessible to enzymes[49]. Residual enzyme activities were low post-hydrolysis. Given their thermal stability, the decrease

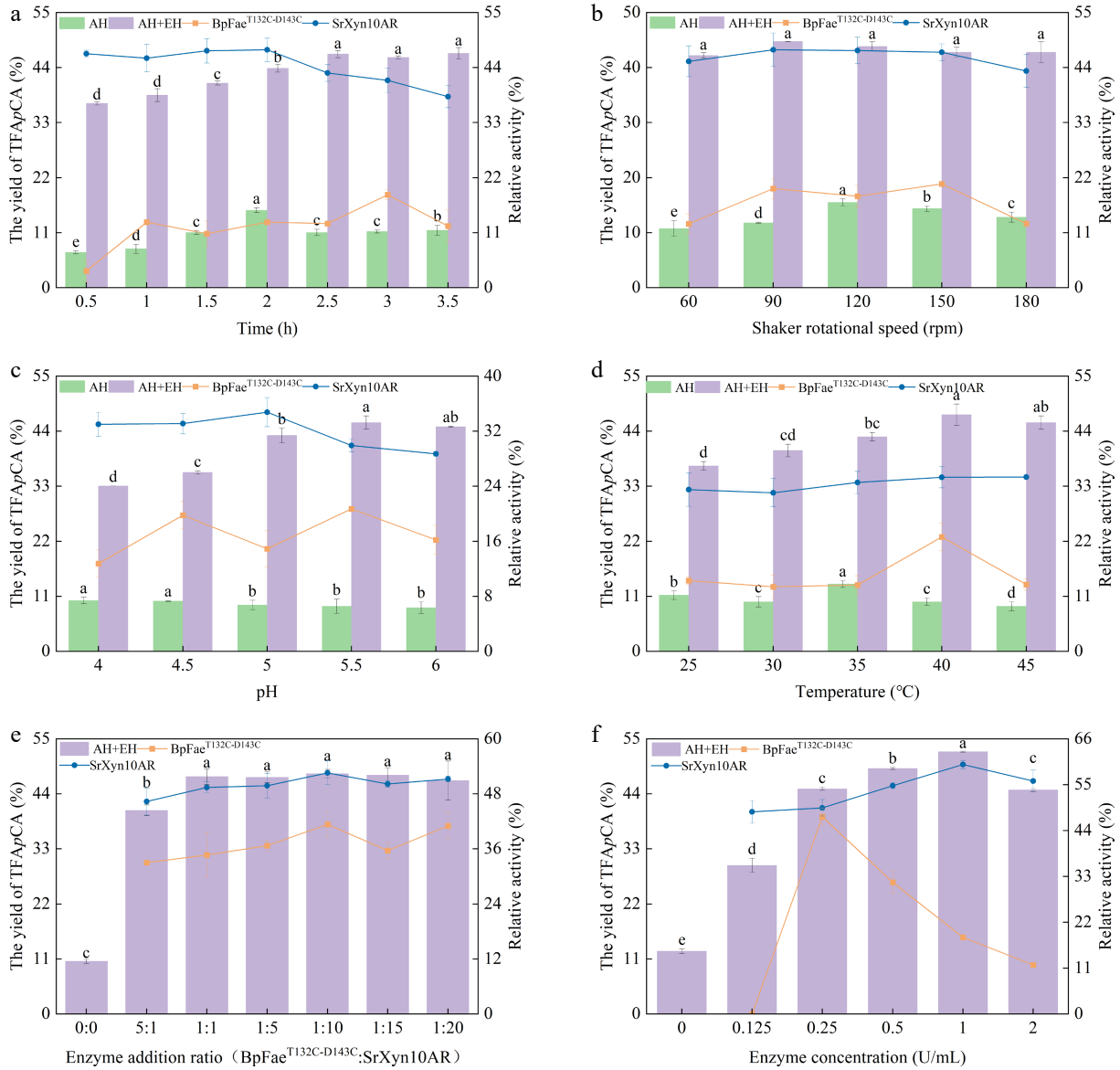

Fig. 2 Effect of (a) time, (b) shaker rotational speed, (c) pH, (d) temperature, (e) enzyme addition ratio, and (f) enzyme concentration on the yield of TFA*p*CA. AH, autohydrolysis only treatment, no enzymatic hydrolysis treatment; AH + EH, autohydrolysis plus enzymatic hydrolysis treatment. Squares, residual enzyme activity of BpFae$^{T132C\text{-}D143C}$; circles, residual enzyme activity of SrXyn10AR.

was mainly attributed to adsorption onto solids and inhibition by complex reaction products[50]. SrXyn10AR maintained high activity during short periods due to thermal stability, but dropped as inhibitors accumulated. BpFae$^{T132C-D143C}$ showed more complex activity fluctuations, influenced by prolonged heating, adsorption-desorption behavior, and modulation by metabolites.

As shown in Fig. 2b, the TFA*p*CA concentration in autohydrolysis liquor supernatant first increased, then decreased with varying rotational speeds. This trend resulted from the release of phenolic acids under optimized autohydrolysis conditions, followed by their partial adsorption onto solid residues. Agitation speed altered the solid–liquid distribution of FA and *p*CA, causing the observed fluctuation. In contrast, enzymatically hydrolyzed samples showed consistent TFA*p*CA levels across speeds, as BpFae$^{T132C-D143C}$ and SrXyn10AR released more free phenolic acids than were adsorbed. Agitation provided sufficient enzyme–substrate contact, while shear effects on enzyme activity remained limited. Residual activity post-hydrolysis varied between enzymes: SrXyn10AR remained stable, while BpFae$^{T132C-D143C}$ first rose then declined. This reflects their differing adsorption behaviors onto residues and shear tolerance under agitation.

As shown in Fig. 2c, the TFA*p*CA concentration in autohydrolyzed corncob residue liquor decreased gradually with increasing pH, likely due to enhanced adsorption of free FA and *p*CA onto residues under alkaline conditions. During enzymatic hydrolysis, TFA*p*CA yield first increased and then slightly decreased with rising pH, aligning with the pH-activity profiles of the two enzymes. BpFae$^{T132C-D143C}$ and SrXyn10AR exhibit optimal activity at pH 4.5–5.0 and pH 6.0, respectively[50], resulting in maximal synergistic efficiency at pH 5.0. Furthermore, this phenomenon was also influenced by the effect of pH on the dissociation state of the substrate[28,48,51]. Residual enzyme activity in the supernatant varied with pH: SrXyn10AR decreased steadily, while BpFae$^{T132C-D143C}$ fluctuated. These patterns reflect the combined effects of pH on enzyme conformation, component ionization, and enzyme adsorption to residual substrates.

After enzymatic hydrolysis at different temperatures, the TFA*p*CA content in the supernatant showed a fluctuating trend with increasing temperature (Fig. 2d), which was closely related to the temperature-dependent distribution of FA and *p*CA between the corncob residue and the solution. The TFA*p*CA yield increased with temperature and reached a maximum of 47.32% at 40 °C, beyond which it slightly decreased. This pattern can be explained by the distinct thermal properties of the two enzymes: SrXyn10AR has higher thermal stability and optimum temperature, while BpFae$^{T132C-D143C}$ has a lower optimum temperature (50 °C) and reduced thermal stability, collectively influencing the efficiency of the co-hydrolysis process. The residual activity of SrXyn10AR remained stable across temperatures, consistent with its reported thermal stability. In contrast, BpFae$^{T132C-D143C}$ showed the highest residual activity at 40 °C. At lower temperatures, although the enzyme's structure remained intact, its weaker degradation capacity led to increased adsorption onto the residue, reducing its activity in the supernatant. At 40 °C, the enzyme's degradation ability improved, promoting its release from the residue into the solution while maintaining structural stability. Further temperature increases, however, likely caused partial denaturation and loss of activity.

As shown in Fig. 2e, enzymatic hydrolysis of autohydrolyzed corncob residue using different ratios of BpFae$^{T132C-D143C}$ and SrXyn10AR significantly increased TFA*p*CA yields compared to the non-enzymatic control. Previous studies indicate that the synergy between xylanases and FAEs enhances agricultural waste degradation, with the enzyme ratio critically influencing this synergistic effect[12]. At a fixed concentration of BpFae$^{T132C-D143C}$, increasing SrXyn10AR concentration raised TFA*p*CA yield to a maximum of 47.44% at a 1:1 ratio, beyond which further increases showed no significant improvement. This is because adequate SrXyn10AR effectively degraded xylan, reducing steric hindrance and allowing BpFae$^{T132C-D143C}$ greater access to phenolic ester bonds. Once most of the degradable xylan was hydrolyzed, additional SrXyn10AR provided no further synergistic benefit[48]. The increase in residual enzyme activity post-hydrolysis further supports enzyme synergy. As substrates were degraded, adsorbed enzymes were released back into solution, elevating measurable activity[52].

As shown in Fig. 2f, with a fixed BpFae$^{T132C-D143C}$ to SrXyn10AR ratio of 1:10, TFA*p*CA yield increased with enzyme concentration and peaked at 48.06% (1 U/mL BpFae$^{T132C-D143C}$ and 10 U/mL SrXyn10AR). Beyond this threshold, yield declined with increasing concentration, which is consistent with the findings of Qin et al.[28] but contrasts with those of Gao et al[53]. Excessive enzymes compete for limited substrate binding sites, lowering hydrolysis efficiency[54,55]. Residual enzyme activities in the supernatant first rose, then declined with increasing concentration. At lower levels, more enzymes were released as substrates degraded; at higher levels, excessive adsorption to non-degradable components (e.g., cellulose and lignin) reduced detectable activity[28]. The differing peak residual activities between the two enzymes reflect variations in substrate composition—xylan vs ferulic acid side chains—affecting their specific and nonspecific adsorption.

RSM

Based on the results of a single-factor experiment, three factors—temperature, time, and enzyme concentration—were chosen to design a Box-Behnken methodology with three levels at the central point, encompassing a total of 15 groups for RSM (Table 3). The highest yield for TFA*p*CA was achieved under the conditions corresponding to the central value levels of the factors.

By conducting multivariate regression analysis on the 15 sets of experimental data and fitting the regression equation, the impact of each factor on the response value can be mathematically represented by the following function:

Table 3. The BBD and the responses of the dependent variables for the enzymatic hydrolysis conditions.

Test No.	Temperature (°C)		Time (h)		Enzyme concentration (U/mL)		Yield of TFA*p*CA (%)
	A	Code A	B	Code B	C	Code C	
1	40	0	2	−1	1.5	1	46.55 ± 0.12
2	45	1	2.5	0	0.5	−1	52.87 ± 0.24
3	40	0	2.5	0	1	0	60.85 ± 0.87
4	40	0	3	1	1.5	1	49.36 ± 0.10
5	45	1	3	1	1	0	53.19 ± 0.53
6	45	1	2.5	0	1.5	1	56.87 ± 0.55
7	40	0	2.5	0	1	0	66.32 ± 0.43
8	40	0	2.5	0	1	0	60.11 ± 0.15
9	35	−1	2.5	0	1.5	1	47.39 ± 0.37
10	35	−1	3	1	1	0	46.33 ± 0.46
11	45	1	2	−1	1	0	51.30 ± 0.12
12	40	0	2	−1	0.5	−1	42.60 ± 0.65
13	35	−1	2	1	1	0	44.20 ± 0.26
14	35	−1	2.5	0	0.5	−1	50.46 ± 0.60
15	40	0	3	1	0.5	−1	46.19 ± 0.51

$$Y = 78.03 + 4.0397A + 1.6285B + 1.2590C - 0.0738AB + 2.2088AC - 0.2455BC - 4.9683A^2 - 12.1228B^2 - 8.1905C^2 \quad (4)$$

where, Y denotes the predicted response (the yield of TFA*p*CA), and A, B, and C represent the factors of temperature, time, and enzyme concentration, respectively.

After analyzing variance, the results showed a pattern with $p < 0.05$, indicating that the model was statistically significant (Supplementary Table S3). Furthermore, the mismatch term was insignificant, as evidenced by a pattern with $p > 0.05$. Additionally, the R^2 value for the regression equation was 0.9875, suggesting a high degree of accuracy for the model. Collectively, these findings indicated that the model can be reliably used to predict the optimal conditions for maximizing the production of TFA*p*CA.

The significance analysis indicated that the primary factors, A (temperature) and B (time), had a substantial impact on production. In contrast, the primary factor C (enzyme concentration) exhibited a relatively minor effect. The order of significance was determined as temperature > time > enzyme concentration. Notably, a significant interaction was observed between temperature and enzyme concentration in relation to their influence on the production of TFA*p*CA. Furthermore, the quadratic terms A^2, B^2, and C^2 were all found to be significant, suggesting a curved (or surface) relationship between temperature, time, and enzyme concentration and the production of TFA*p*CA.

Three-dimensional plots derived from the fitted equation clearly demonstrated that the yield of TFA*p*CA initially increased and then decreased as both the time and enzyme concentration increased (Supplementary Fig. S2). In contrast, as the temperature incrementally rose, its impact demonstrated an initial upward trend followed by a slight decline. From this observation, it can be deduced that, within the tested spectrum of factor levels, the time and enzyme concentration were situated roughly around their median values, whereas the temperature leaned slightly towards the upper limit of the range. This indicated that the yield of TFA*p*CA followed a parabolic trend as the temperature, time, or concentration increased, achieving maximum yield at appropriate levels of these factors.

Using Design-Expert 11 software, the optimal conditions for maximizing TFA*p*CA yield were determined. The model predicted a maximum yield of 61.53% at 43 °C, 2.5 h, and a BpFae$^{T132C-D143C}$ concentration of 1.1 U/mL. Validation experiments under these optimal conditions (with additional fixed parameters: 90 rpm shaker speed, pH 5.5, and SrXyn10AR concentration of 1.1 U/mL) yielded 63.42%, a value close to the prediction, confirming the model's accuracy and effectiveness. This value closely approximated the current highest yield of FA extracted from corncob, standing at 67.70%[10], and exceeds the yield documented in other research endeavors[34,35] (Table 4). Notably, the time used in this study is significantly shorter, only one-tenth of that required to achieve the highest previously reported yield, markedly improving production efficiency. Furthermore, this study investigated the yield of two phenolic acids, specifically including *p*CA, further demonstrating the high efficacy of BpFae$^{T132C-D143C}$.

Production of TFA*p*CA from enzymatically pretreated corncob utilizing various enzymatic methods

Under optimized conditions, TFA*p*CA yields were assessed from autohydrolyzed corncob residues treated with BpFae$^{T132C-D143C}$ alone, SrXyn10AR alone, or their combination. As shown in Supplementary Fig. S3, SrXyn10AR alone only moderately increased TFA*p*CA yield (42.43% over the untreated sample), indicating its primary activity toward xylan rather than phenolic acid ester bonds. In contrast, BpFae$^{T132C-D143C}$ alone markedly raised TFA*p*CA yield to 52.51%—a 305.80% increase—demonstrating high specificity and efficiency in releasing FA and *p*CA, outperforming its parental enzyme BpFae on wheat bran[51]. This difference may stem from substrate composition, pretreatment, and the mutant's catalytic properties. The enzyme combination, optimized with more BpFae$^{T132C-D143C}$, proved highly effective, achieving a 64.08% TFA*p*CA yield (395.20% increase over untreated). This result exceeded the sum of individual enzyme effects, confirming a synergistic interaction between BpFae$^{T132C-D143C}$ and SrXyn10AR in enhancing phenolic acid release, consistent with prior reports[56].

Table 4. Summary of representative FA productions from corncob.

Total FA content (mg/g)	Feruloyl esterase concentration	Xylanase concentration	Time (h)	Yield of FA (%)	Ref.
18.8	0.04 U/mL		24	9.63	[35]
		4 U/mL		4.31	
	0.04 U/mL	4 U/mL		14.89	
10.13	0.8 mg/mL	–	1	43.24	[34]
10.78	46 μg/mL	46 μg/mL	24	67.70	[10]
17.85 (FA) and 11.29 (*p*CA)	1.1 U/mL	1.1 U/mL	2.5	63.42 (TFA*p*CA)	In this study

Sugars composition

Under optimal autohydrolysis and enzymatic hydrolysis conditions, analysis revealed the presence of XOS with varying degrees of polymerization (DP), along with xylose, arabinose, and glucose (Supplementary Fig. S4 and Supplementary Table S4). This indicates that autohydrolysis effectively cleaves hemicellulose and cellulose to generate diverse XOS while releasing limited monosaccharides, consistent with previous reports[29,37]. However, individual XOS (DP 2–6) content remained relatively low (≤ 20 mg/g), with total XOS yield below 57.96 mg/g. Subsequent dual-enzyme hydrolysis using SrXyn10AR and BpFae$^{T132C-D143C}$ significantly increased XOS yields, with all types rising over 200%. Xylobiose (32.26 mg/g) and xylotriose (47.26 mg/g) increased by 561.18% and 628.14%, respectively, bringing the total XOS yield to 303.31 mg/g—5.23 times that after autohydrolysis. This confirms efficient hydrolysis of autohydrolyzed corncob residue by the synergistic action of the two enzymes. In addition to facilitating substantial TFA*p*CA release, the process generated considerable XOS. The marked increase in xylobiose and xylotriose aligns with the known enzymatic specificity of SrXyn10AR, which predominantly yields these oligosaccharides during xylan hydrolysis[22,50]. Furthermore, the potential auxiliary function of BpFae$^{T132C-D143C}$ in this process cannot be overlooked. Concurrently, modest increases in xylose (28.98%) and arabinose (19.88%) were observed, consistent with the reported activity of SrXyn10AR in producing minor amounts of xylose[57] and the concomitant degradation of arabinose side chains. In contrast, glucose levels remained stable, attributable to the substrate selectivity of both enzymes toward non-cellulosic components. Although autohydrolysis may expose some cellulose, neither enzyme can degrade cellulose, leaving glucose content unaffected. In conclusion, treating autohydrolyzed corncob with BpFae$^{T132C-D143C}$ and SrXyn10AR not only enhances the production of FA and *p*CA but also enables high XOS yields. While the current conditions may not be optimal for XOS production alone, further optimization could be applied to the residue after preferential recovery of phenolic acids. This stepwise valorization strategy enables full component utilization of agricultural waste, maximizing its economic potential.

Morphological structure of corncob after various pretreatments

SEM analyzed structural changes in untreated, autohydrolyzed, and enzymatically hydrolyzed corncob (Fig. 3). The untreated sample showed a smooth, compact surface with no fractures, indicating a dense lignocellulosic structure that hinders enzymatic action (Fig. 3a). After autohydrolysis, the surface became rough and porous, with visible cracks and holes, reflecting breakdown of the rigid framework and cleavage of lignin–carbohydrate linkages, which enabled hemicellulose degradation into XOS and monosaccharides (Fig. 3b). This porous structure improved enzyme accessibility. Subsequent enzymatic hydrolysis further disrupted the morphology, resulting in extensive fragmentation and a rougher surface, indicating hemicellulose conversion into FA, *p*CA, and sugars, leaving fragmented cellulose (Fig. 3c). These pronounced structural changes confirm the efficacy of the dual-enzyme treatment, consistent with previous studies[28,38,58].

FTIR spectroscopy analysis

FTIR analysis compared untreated corncob, autohydrolyzed corncob, and enzymatically hydrolyzed corncob. Although specific bands differed, overall spectral profiles were similar (Fig. 4). A broad band around 3,340 cm^{-1} in all samples, assigned to O–H stretching in cellulose and hemicellulose, showed reduced intensity after autohydrolysis and enzymatic hydrolysis, indicating partial disruption of hydrogen bonding[28,59]. The peak near 2,930 cm^{-1}, attributed to C–H stretching in lignin and polysaccharides, decreased after autohydrolysis and further weakened with a blue shift after enzymatic hydrolysis, suggesting degradation of these components[28,59]. The band around 1,710 cm^{-1}, associated with C=O stretching in acetyl and ester groups (hemicellulose and lignin), decreased and redshifted following treatments, confirming breakage of ester linkages[28,59,60]. Bands at 1,603 cm^{-1} (lignin acetyl vibration) and 1,515 cm^{-1} (lignin aromatic vibration) changed with treatments: 1,603 cm^{-1} increased slightly after autohydrolysis, likely due to exposed acetyl groups, while 1,515 cm^{-1} rose after autohydrolysis but dropped after enzymatic hydrolysis, indicating lignin alteration and degradation[28,59,60]. Minor bands between 1,453–1,250 cm^{-1}, representing C–O, C=O, and C–H vibrations in hemicellulose and lignin, also decreased after treatments, suggesting hemicellulose damage[28,38,59]. The peak at 898 cm^{-1}, indicating β-glycosidic bonds in cellulose/hemicellulose, declined post-treatment, confirming polysaccharide degradation[59]. In summary, both autohydrolysis and enzymatic hydrolysis successfully disrupted the major components of corncob. The pronounced attenuation of specific peaks, especially those related to ester bonds, post-enzymatic hydrolysis correlates with the release of FA, *p*CA, and XOS into the hydrolysate.

Conclusions

In summary, this study achieved a significant breakthrough by optimizing the process conditions for treating corncob through autohydrolysis in conjunction with the synergistic action of FAE $BpFae^{T132C\text{-}D143C}$ and xylanase SrXyn10AR. The optimized conditions included a heat treatment at 165 °C for 34 min, a solid-to-liquid ratio of 1:90.8, and the use of corncob particles with a size between 40–60 mesh. Following this, a dual-enzyme hydrolysis process was carried out at 43 °C and pH 5.5 for 2.5 h, with a shaker speed maintained at 90 rpm and both enzymes added at a concentration of 1.1 U/mL. Under these refined conditions, the yield of TFA*p*CA was notably elevated, achieving a 2.4-fold increase compared to the unoptimized conditions, reaching a total yield of 63.42%. Furthermore,

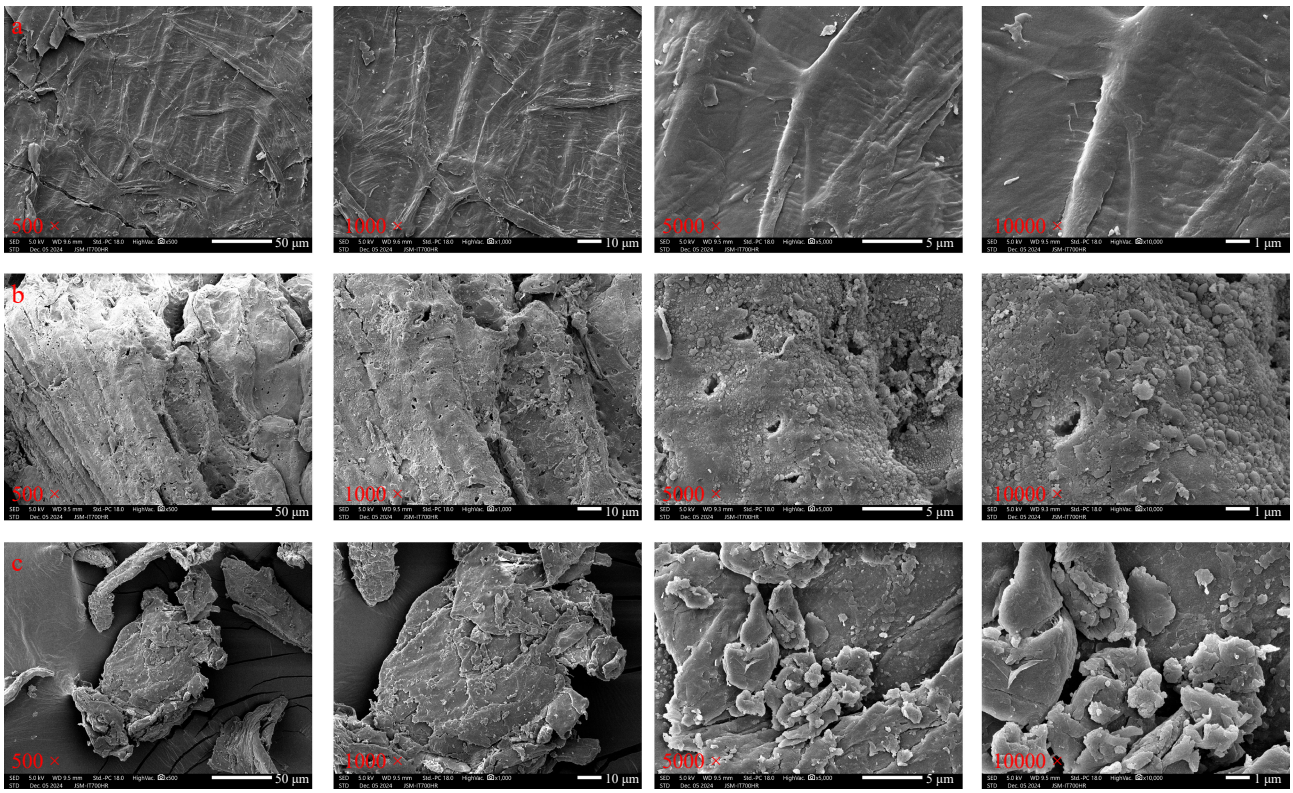

Fig. 3 SEM of (a) corncob, (b) corncob after autohydrolysis treatment, and (c) corncob after autohydrolysis and enzymatic hydrolysis treatments. Scale bars: 500 μm (500 ×), 10 μm (1,000 ×), 5 μm (5,000 ×), 1 μm (10,000 ×).

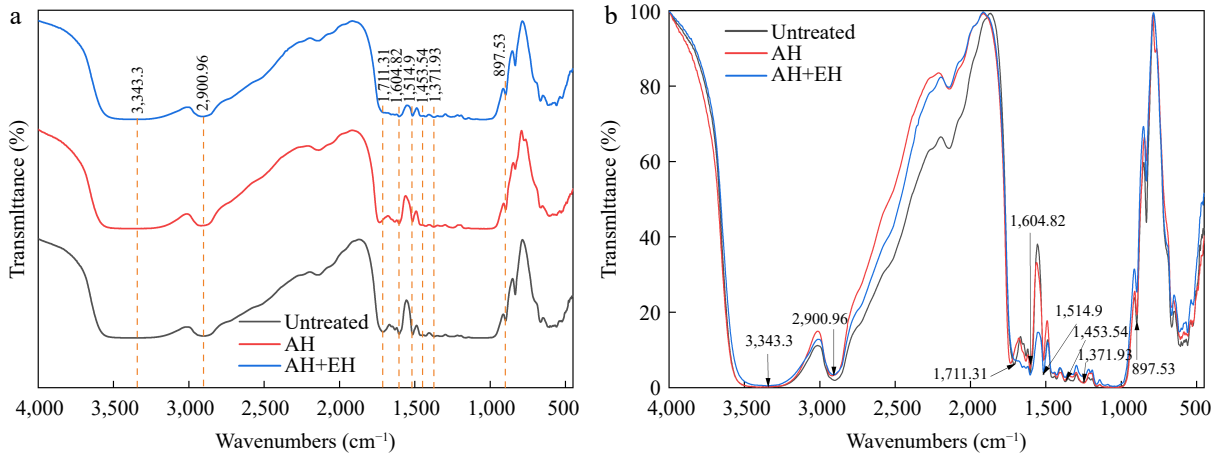

Fig. 4 FTIR spectra of corncob (untreated), corncob after autohydrolysis treatment (AH), and corncob after autohydrolysis and enzymatic hydrolysis treatments (AH+EH). AH, autohydrolysis only treatment, no enzymatic hydrolysis treatment; AH+EH, autohydrolysis plus enzymatic hydrolysis treatment.

the residual activities of the enzymes post-hydrolysis were assessed, and XOS production quantified under the optimal treatment conditions. The comprehensive analysis of the results underscores that the integration of autohydrolysis with SrXyn10AR and BpFae$^{T132C\text{-}D143C}$ not only markedly enhances the economic potential of corncob but also offers a viable and environmentally friendly approach for the efficient production of high-value-added compounds such as FA, *p*CA, and XOS.

Author contributions

The authors confirm contribution to the paper as follows: investigation: study conception and design: Ma J, Liu X, Fan G; methodology: Ma J, Cui W, Chen M; writing – original draft: Ma J; writing – review and editing: Liu X, Basit RA, Fu Z, Fan G; data curation: Gao P; resources, supervision: Xiao L, Yan J, Liu Y, Fan G. All authors reviewed the results and approved the final version of the manuscript.

Data availability

The datasets generated during and/or analyzed during the current study are available from the corresponding author on reasonable request.

Acknowledgments

This research was supported by Beijing Natural Science Foundation (Grant No. 6222003) and Open Research Fund Program of Guangxi Key Lab of Agricultural Resources Chemistry and Biotechnology (Grant No. 2024KF05).

Conflict of interest

The authors declare that they have no conflict of interest.

Supplementary information accompanies this paper online at: https://doi.org/10.48130/fia-0026-0002.

Dates

Received 30 May 2025; Revised 7 January 2026; Accepted 7 January 2026; Published online 2 March 2026

References

[1] Antunes FAF, Freitas JBF, Prado CA, Castro-Alonso MJ, Diaz-Ruiz E, et al. 2023. Valorization of corn cobs for xylitol and bioethanol production through column reactor process. *Energies* 16:4841

[2] Echeverría-Pérez J, Carvajal-Palacio W, Gómez-Plata L, Vacca-Jimeno V, Cubillán N. 2023. Corn cobs and KOH-treated biomasses for indigo carmine removal: kinetics and isotherms. *Emergent Materials* 6(4):1217–1229

[3] Gandam PK, Chinta ML, Pabbathi NPP, Baadhe RR, Sharma M, et al. 2022. Second-generation bioethanol production from corncob - a comprehensive review on pretreatment and bioconversion strategies, including techno-economic and lifecycle perspective. *Industrial Crops and Products* 186:115245

[4] Salgado JM, Rodríguez-Solana R, Curiel JA, de las Rivas B, Muñoz R, et al. 2012. Production of vinyl derivatives from alkaline hydrolysates of corn cobs by recombinant *Escherichia coli* containing the phenolic acid decarboxylase from *Lactobacillus plantarum* CECT 748T. *Bioresource Technology* 117:274–285

[5] Wei YM, Chen K, Kang JN, Chen W, Wang XY, et al. 2022. Policy and management of carbon peaking and carbon neutrality: a literature review. *Engineering* 14:52–63

[6] Arumugam A, Malolan V V, Ponnusami V. 2021. Contemporary pretreatment strategies for bioethanol production from corncobs: a comprehensive review. *Waste and Biomass Valorization* 12(2):577–612

[7] Rivas B, Domínguez JM, Domínguez H, Parajó JC. 2002. Bioconversion of posthydrolysed autohydrolysis liquors: an alternative for xylitol production from corn cobs. *Enzyme and Microbial Technology* 31(4):431–438

[8] McCann MC, Carpita NC. 2015. Biomass recalcitrance: a multi-scale, multi-factor, and conversion-specific property. *Journal of Experimental Botany* 66(14):4109–4118

[9] Nirwana WOC, Hung IH, Shu CH. 2023. Enhancing the bioconversion of ferulic acid from alkaline hydrolysate of corn cobs to vanillin by *Amycolatopsis thermoflava* under nutrient limitation and reducing sugar control. *Journal of Chemical Technology and Biotechnology* 98(1):238–246

[10] Wang R, Yang J, Jang JM, Liu J, Zhang Y, et al. 2020. Efficient ferulic acid and xylo-oligosaccharides production by a novel multi-modular bifunctional xylanase/feruloyl esterase using agricultural residues as substrates. *Bioresource Technology* 297:122487

[11] Pérez-Rodríguez N, Torrado Agrasar A, Domínguez JM. 2017. High hydrostatic pressure as pretreatment and adjuvant for the enzymatic release of ferulic acid from corn cob. *Process Biochemistry* 58:204–210

[12] Lau T, Harbourne N, Oruña-Concha MJ. 2020. Optimization of enzyme-assisted extraction of ferulic acid from sweet corn cob by response

surface methodology. *Journal of the Science of Food and Agriculture* 100(4):1479–1485

[13] Zhang J, Tang H, Yu X, Xue D, Li M, et al. 2024. Co-production of ferulic acid and p-coumaric acid from distiller grain by a putative feruloyl esterase discovered in metagenome assembled genomes. *Journal of Cleaner Production* 439:140814

[14] Cao L, Xue D, Liu X, Wang C, Fang D, et al. 2023. Ferulic acid production from wheat bran by integration of enzymatic pretreatment and a cold-adapted carboxylesterase catalysis. *Bioresource Technology* 385:129435

[15] Ferri M, Happel A, Zanaroli G, Bertolini M, Chiesa S, et al. 2020. Advances in combined enzymatic extraction of ferulic acid from wheat bran. *New Biotechnology* 56:38–45

[16] Qian S, Gao S, Li J, Liu S, Diao E, et al. 2022. Effects of combined enzymatic hydrolysis and fed-batch operation on efficient improvement of ferulic acid and p-coumaric acid production from pretreated corn straws. *Bioresource Technology* 366:128176

[17] Santiago R, Barros-Rios J, Malvar RA. 2013. Impact of cell wall composition on maize resistance to pests and diseases. *International Journal of Molecular Sciences* 14:6960–6980

[18] Mkabayi L, Malgas S, Wilhelmi BS, Pletschke BI. 2020. Evaluating feruloyl esterase-xylanase synergism for hydroxycinnamic acid and xylo-oligosaccharide production from untreated, hydrothermally pre-treated and dilute-acid pre-treated corn cobs. *Agronomy* 10(5):688

[19] Van Dyk JS, Pletschke BI. 2012. A review of lignocellulose bioconversion using enzymatic hydrolysis and synergistic cooperation between enzymes-Factors affecting enzymes, conversion and synergy. *Biotechnology Advances* 30(6):1458–1480

[20] Oliveira DM, Mota TR, Oliva B, Segato F, Marchiosi R, et al. 2019. Feruloyl esterases: Biocatalysts to overcome biomass recalcitrance and for the production of bioactive compounds. *Bioresource Technology* 278:408–423

[21] Ma J, Basit R A, Yuan S, Zhao X, Liu X, et al. 2025. Optimization of fermentation conditions for the production of recombinant feruloyl esterase BpFae$^{T132C\text{-}D143C}$. *Folia Microbiologica* 70:441–454

[22] Fan G, Wu Q, Li Q, Sun B, Ma Y, et al. 2020. Impact of the disulfide bond on hydrolytic characteristics of a xylanase from *Talaromyces thermophiles* F1208. *International Journal of Biological Macromolecules* 164:1748–1757

[23] Yang R, Li J, Teng C, Li X. 2016. Cloning, overexpression and characterization of a xylanase gene from a novel *Streptomyces rameus* L2001 in *Pichia pastoris*. *Journal of Molecular Catalysis B: Enzymatic* 131:85–93

[24] Bailey MJ, Biely P, Poutanen K. 1992. Poutanen, Interlaboratory testing of methods for assay of xylanase activity. *Journal of Biotechnology* 23(3):257–270

[25] Standardization Administration of China. 2011. *General methods of analysis for Daqu (QB/T 4257-2011)* (in Chinese). Beijing, China: Standards Press of China. https://std.samr.gov.cn/hb/search/stdHBDetailed?id=8B1827F1AF6FBB19E05397BE0A0AB44A

[26] AOAC International. 2016. *Official methods of analysis of AOAC International*. 20th Edition, AOAC International, Rockville. www.eoma.aoac.org

[27] Sluiter A, Hames B, Ruiz R O, Scarlata C, Templeton D. 2004. Determination of structural carbohydrates and lignin in biomass. *Laboratory analytical procedure* 1617(1):1–16

[28] Qin L, Ma J, Tian H, Ma Y, Wu Q, et al. 2022. Production of xylooligosaccharides from Jiuzao by autohydrolysis coupled with enzymatic hydrolysis using a thermostable xylanase. *Foods* 11(17):2663

[29] Qin L, Liu X, Wu Q, Tian H, Ma Y, et al. 2022. Combining autohydrolysis with xylanase hydrolysis for producing xylooligosaccharides from *Jiuzao*. *Biochemical Engineering Journal* 187:108678

[30] Jiang K, Li L, Long L, Ding S. 2018. Comprehensive evaluation of combining hydrothermal pretreatment (autohydrolysis) with enzymatic hydrolysis for efficient release of monosaccharides and ferulic acid from corn bran. *Industrial Crops and Products* 113:348–357

[31] de Mello Capetti CC, Pellegrini VOA, Espirito Santo MC, Cortez AA, Falvo M, et al. 2023. Enzymatic production of xylooligosaccharides from corn cobs: Assessment of two different pretreatment strategies. *Carbohydrate Polymers* 299:120174

[32] Xia W, Li F, Chang Y, Jiang Y, Shen Y. 2014. Production of ferulic acid and p-cumaric acid from corn cob by alkaline hydrolysis. *Journal of Anhui Agricultural Sciences* 42(29):10302–10305

[33] Zhang T, Zhang S, Lan W, Yue F. 2023. Quantitative extraction of p-coumaric acid and ferulic acid in different gramineous materials and structural changes of residual alkali lignin. *Journal of Renewable Materials* 11(2):555–566

[34] Zhang R, Lin D, Zhang L, Zhan R, Wang S, et al. 2022. Molecular and biochemical analyses of a novel trifunctional endoxylanase/endoglucanase/feruloyl esterase from the human colonic bacterium *Bacteroides intestinalis* DSM 17393. *Journal of Agricultural and Food Chemistry* 70(13):4044–4056

[35] Li XY, Duan YT, Wu L, Mo WJ, Zhou JG, et al. 2020. High-efficient secretory expression of feruloyl esterase A in *Kluyveromyces marixanus* via the combination of genomic integration and episomal plasmid. *Journal of Fudan University(Natural Science)* 59(05):608–617

[36] Liang T, Li S, Ou S. 2011. Preparation of p-coumaric acid and xylo-oligosaccharides from corn cob. *Science and Technology of Food Industry* 32(12):341–344

[37] Zhang W, You Y, Lei F, Li P, Jiang J. 2018. Acetyl-assisted autohydrolysis of sugarcane bagasse for the production of xylo-oligosaccharides without additional chemicals. *Bioresource Technology* 265:387–393

[38] Qian S, Guan T, Li L, Diao E, Fan J, et al. 2023. Efficient production of ferulic acid and p-coumaric acid from reed straws via combined enzymatic hydrolysis and hydrothermal pretreatment. *Food and Bioproducts Processing* 140:122–131

[39] Álvarez C, González A, Negro MJ, Ballesteros I, Oliva JM, et al. 2017. Optimized use of hemicellulose within a biorefinery for processing high value-added xylooligosaccharides. *Industrial Crops and Products* 99:41–48

[40] Surek E, Buyukkileci AO, Yegin S. 2021. Processing of hazelnut (*Corylus avellana* L.) Shell autohydrolysis liquor for production of low molecular weight xylooligosaccharides by *Aureobasidium pullulans* NRRL Y-2311-1 xylanase. *Industrial Crops and Products* 161:113212

[41] Saad S, Dávila I, Mannai F, Labidi J, Moussaoui Y. 2024. Effect of the autohydrolysis treatment on the integral revalorisation of *Ziziphus lotus*. *Biomass Conversion and Biorefinery* 14(2):1413–1425

[42] Valério R, Serra AT, Baixinho J, Cardeira M, Fernández N, et al. 2021. Combined hydrothermal pre-treatment and enzymatic hydrolysis of corn fibre: Production of ferulic acid extracts and assessment of their antioxidant and antiproliferative properties. *Industrial Crops and Products* 170:113731

[43] Fang L, Su Y, Wang P, Lai C, Huang C, et al. 2022. Co-production of xylooligosaccharides and glucose from birch sawdust by hot water pretreatment and enzymatic hydrolysis. *Bioresource Technology* 348:126795

[44] Morales PC, García-Martín A, Ladero M. 2023. Pectooligosaccharides rich in galacturonic acid produced from orange processing waste by autohydrolysis: Process optimization and kinetic analysis. *Bioresource Technology Reports* 21:101369

[45] Zheng B, Zhu Y, Zheng S, Mo Y, Sun S, et al. 2021. Upgrade the torrefaction process of bamboo based on autohydrolysis pretreatment. *Industrial Crops and Products* 166:113470

[46] Jiang Y, Xing M, Kang Q, Sun J, Zeng XA, et al. 2022. Pulse electric field assisted process for extraction of Jiuzao glutelin extract and its physicochemical properties and biological activities investigation. *Food Chemistry* 383:132304

[47] Jiang Y, Sun J, Yin Z, Li H, Sun X, et al. 2020. Evaluation of antioxidant peptides generated from Jiuzao (residue after Baijiu distillation) protein hydrolysates and their effect of enhancing healthy value of Chinese Baijiu. *Journal of the Science of Food and Agriculture* 100(1):59–73

[48] Wang YS, Zhu X, Jin LQ, Zheng Y, Liao CJ, et al. 2017. Post-hydrolysis of the prehydrolysate from eucalyptus pulping with xylanase. *Journal of Cleaner Production* 142:2865–2871

[49] Zeng Y, Yu HJ, Yang B, Yin X, Wu MC. 2015. Synergistic effect of feruloyl esterase and cellulase on the release of ferulic acid from wheat bran. *Journal of Food Science and Biotechnology* 34(04):379–384

[50] Wu Q, Zhang C, Zhu W, Lu H, Li X, et al. 2023. Improved thermostability, acid tolerance as well as catalytic efficiency of *Streptomyces rameus* L2001 GH11 xylanase by N-terminal replacement. *Enzyme and Microbial Technology* 162:110143

[51] Fu Z, Zhu Y, Teng C, Fan G, Li X. 2021. Biochemical characterization of a novel feruloyl esterase from *Burkholderia pyrrocinia* B1213 and its application for hydrolyzing wheat bran. *3 Biotech* 12(1):24

[52] Wu H, Li H, Xue Y, Luo G, Gan L, et al. 2017. High efficiency co-production of ferulic acid and xylooligosaccharides from wheat bran by recombinant xylanase and feruloyl esterase. *Biochemical Engineering Journal* 120:41–48

[53] Gao P, Ma J, Basit RA, Lou X, Zhang W, et al. 2025. Investigation of the enzymatic characteristics of thermotolerant xylanase McXyn0243 derived from *Malbranchea cinnamomea*, and its application in the degradation of three agricultural residues for the production of xylooligosaccharides. *International Journal of Biological Macromolecules* 313:143973

[54] Mazlan NA, Samad KA, Wan Yussof H, Saufi SM, Jahim J. 2019. Xylooligosaccharides from potential agricultural waste: characterization and screening on the enzymatic hydrolysis factors. *Industrial Crops and Products* 129:575–584

[55] Yu Q, Liu J, Zhuang X, Yuan Z, Wang W, et al. 2016. Liquid hot water pretreatment of energy grasses and its influence of physico-chemical changes on enzymatic digestibility. *Bioresource Technology* 199:265–270

[56] Cerullo G, Varriale S, Bozonnet S, Antonopoulou I, Christakopoulos P, et al. 2019. Directed evolution of the type C feruloyl esterase from *Fusarium oxysporum* FoFaeC and molecular docking analysis of its improved variants. *New Biotechnology* 51:14–20

[57] Wu Q, Zhang C, Dong W, Lu H, Yang Y, et al. 2023. Simultaneously enhanced thermostability and catalytic activity of xylanase from *Streptomyces rameus* L2001 by rigidifying flexible regions in loop regions of the N-terminus. *Journal of Agricultural and Food Chemistry* 71(34):12785–12796

[58] Ladeira Ázar RIS, Bordignon-Junior SE, Laufer C, Specht J, Ferrier D, et al. 2020. Effect of lignin content on cellulolytic saccharification of liquid hot water pretreated sugarcane bagasse. *Molecules* 25(3):623

[59] Gong L, Feng D, Liu J, Yu Y, Wang J. 2022. Ionic liquid depolymerize the lignocellulose for the enzymatic extraction of feruloylated oligosaccharide from corn bran. *Food Chemistry: X* 15:100381

[60] Nitsos CK, Matis KA, Triantafyllidis KS. 2013. Optimization of hydrothermal pretreatment of lignocellulosic biomass in the bioethanol production process. *ChemSusChem* 6(1):110–122